Journal of Applied Pharmaceutical Science Vol. 14(09), pp 169-181, September, 2024
Available online at http://www.japsonline.com
DOI: 10.7324/JAPS.2024.184768
ISSN 2231-3354

# An evaluation of *Sargassum cinctum* anticancer properties utilizing *in vitro* testing and molecular docking, with assistance from GC-HRMS and FTIR

Mohini Salunke[1*], Preeti Mane[2], Smita Kumbhar[3], Balaji Wakure[1]

[1]Vilasrao Deshmukh Foundation, Group of Institutions, VDF School of Pharmacy, Latur, India.
[2]Department of Pharmacy, Terna Public Charitable Trust's, College of Engineering, Dharashiv, India.
[3]DSTS Mandal's College of Pharmacy, Solapur, India.

**ARTICLE HISTORY**

Received on: 10/04/2024
Accepted on: 06/08/2024
Available Online: 05/09/2024

***Key words:***
*Sargassum cinctum,* GC-HRMS, FT-IR, anticancer, docking studies.

**ABSTRACT**

Cancer is characterised by unregulated, uncontrollable cell development, which is a continuous abnormality in cellular behavior. This frequently results in the aggressive invasion, metastasis, and dispersal of malignant cells throughout different organs. Breast cancer is one of the most common types of cancer that is prevalent worldwide. In particular, it comes in second place after lung cancer in terms of cancer-related mortality among women. The current work concentrated on identifying bioactive components in ethanolic extracts of *Sargassum cinctum* by gas chromatography high-resolution mass spectroscopy (GC-HRMS) and Fourier-transformed infrared (FTIR) analysis. Following GC-HRMS and FT-IR studies, anticancer activity and molecular docking are carried out on the ethanolic extract of *S. cinctum*. Different bioactive compounds, including phenols, alcohols, amines, aldehydes, ketone esters, carboxylic acids, alkenes, and alkanes, are detected by the GC-HRMS and FT-IR analyses. *Sargassum cinctum* ethanolic extract exhibits strong anti-cancer properties. The $IC^{50}$ value of the MCF 7 cell line and A549 cell line is 134.50 and 161.02 µg/ml, respectively. Asn923, Phe1047, Lys868, and Asp1046 from vascular endothelial growth factor receptor (VEGFR) and Met623, Asp690, and Lys567 from anexelekto (AXL) kinase are among the residues that may have contributed to the anti-cancer benefit observed in this study. Using *in-silico* approach, it was determined that the medications that target the VEGFR2 and AXL kinase receptors had anticancer properties. This is the first-hand evaluation of the bioactive elements of *S. cinctum* extracts that have anticancer potential, as far as we aware. Recent study proved value of *in silico* analyses in the search for new drugs and the capacity of marine compounds to produce distinctive bioactives with considerable biological activity.

## INTRODUCTION

Every year, millions of new people receive a cancer diagnosis, and the disease also claims many lives, making it a serious health issue [1,2]. According to estimates from the International Agency for Research on Cancer, there were 8.2 million cancer-related deaths and 14 million new cases of the disease worldwide in 2012. An estimated 22 million additional instances of cancer and 13 million cancer-related deaths per year are predicted by 2030, assuming the aging and growing global population. The cancer burden in the future will likely be significantly greater in economically developing nations because of alterations in living factors, including being inactive, smoking, having fewer births, and eating poorly [3].

The globe, one of the most serious diseases is cancer and chemotherapy for cancer is the greatest treatment option. Almost all the anticancer drugs used in chemotherapy are harmful to healthy cells [4].

In terms of the frequency of malignant tumors in women, breast cancer (BC) is ranked second worldwide. BC is

*Corresponding Author
*Mohini Salunke, Vilasrao Deshmukh Foundation, Group of Institutions, VDF School of Pharmacy, Latur, India.*
*E-mail: mohinisalunke82 @ gmail.com*

the most common type of cancer that kills women globally. BC cases have grown, going from 1.7 million in 2005–2.4 million in 2015 [5].

Lung cancer, which has a mortality rate of 30.0 per 100,000 people aged and is a primary global cause of cancer-related fatalities in both men and women, and the efficacy of available treatments is severely hampered [6].

Traditional remedies have been treating and preventing many ailments using herbs for ages. Several anticancer medications used in clinical settings, including paclitaxel, vinblastine, and camptothecin, are derived from plants. Due to the many environmental factors in marine settings, there is a vast supply of potentially bioactive substances that are generally well tolerated by humans and have minimal adverse effects [7].

A variety of marine species have reported producing over 2,500 novel metabolites. One of them, Seaweed, a kind of marine plant, sticks to the seafloor in rather shallow coastal waters. These were less complicated than flowering plants since they do not have real leaves, roots, flowers, or seeds. The colors, shapes, structural complexity, and sizes of seaweeds vary despite these structural restrictions. In the world's marine environments, more than 1.5 million different types of seaweed exist, yet only a small number have been recognized and used by humans [8].

Seaweeds are one of the marine ecosystem's natural food sources, as well as a source of bioactive substances such as medications and diagnostic aids. The various seaweeds of subtropical and tropical regions have produced around 2,400 naturally occurring marine products that are used as food, fodder, fertilizer, and medicines [9].

Like terrestrial plants, macroalgae use photosynthesis to create their nutrition when both seawater and sunshine are present. Along the coast, seaweed has become well-established and is found in regions where the tide is high and low. They include a variety of pigment kinds. Fucoxanthin in Phaeophyta (brown algae), phycoerythrin and phycocyanin in Rhodophyta (red algae), and chlorophyll pigment are found in Chlorophyta (green algae) [10].

The *Sargassum* is known for its planktonic, many species of brown algae that often exist in temperate and tropical climates. The literature review indicates that *Sargassum* species are prospective sources of a variety of kinds of secondary metabolites, including chromanols, plastoquinones, steroids, chromenes, and glycerides which show antioxidant, antibacterial, anticancer, antifungal, antiallergic, anti-inflammatory anti-herpes, antihistamine, hepatoprotective, and anticholinergic properties [11].

Today's cancer treatments are harmful and expensive since they damage both healthy and cancerous cells. Finding new, potent, and non-toxic chemicals from natural origin is, therefore, more important than ever [12].

Cytarabine, eribulin mesylate, and trabectedin are only a few of the sea-based anticancer medications that have received FDA approval. This has caused the pharmaceutical industry to concentrate on marine-based natural products, and several marine bioactives have entered preclinical and clinical testing [13,14].

One of the frequently identified kinases linked to the emergence of several cancer types is anexelekto (AXL) receptor tyrosine kinase. Tyro3 and Mer are two more TAM family receptors in addition to AXL [15]. As with the other TAM members, the growth arrest-specific protein 6 ligand interacts with AXL to activate it. The receptor is a possible contributor to several oncogenic processes. Invasion, migration, survival, angiogenesis, cell transformation, and proliferation are just a few of the critical biological processes that AXL signalization supports for the development and spread of cancer. AXL overexpression or increased activity has been linked to metastasis in several cancer types, and it is indicative of a poor prognosis for the patients [16]. Because AXL tyrosine kinase is highly expressed in a variety of cancer cell lines, it is a desirable target for the development of anti-cancer drugs [15,17].

The development, survival, and metastasis of tumors all depend on the process of tumor angiogenesis. Angiogenesis is regulated by many pro-and anti-angiogenic molecules and signaling pathways [18], which promote tumor development and spread. The main mechanism that stimulates angiogenesis is the signalling of the vascular endothelial growth factor receptor 2 (VEGFR2) [19].

Molecular docking and synergism are two recent ideas for successful drug discovery; however, none of these can fully offset the importance of natural ingredients in the creation of pharmaceuticals [20].

For the purpose of observing functional groups and identifying the many bioactive chemicals found in plants, Gas chromatography-mass spectrometry (GC-MS) and Fourier-transformed infrared (FTIR) have been extensively employed [21].

Molecular docking is a fast, low-cost approach to drug development and testing. In order to predict how the drug's target proteins would bind in the model, this method gives information about potential drug-receptor interactions. This leads to a reliable interaction at the ligands' binding sites [22].

To the extent of our information, there is not a publication that discusses the existence and evaluation of several bioactive components in the *S. cinctum*. Therefore, the current work concentrated on identifying bioactive components in ethanolic extracts of *S. cinctum* by gas chromatography high-resolution mass spectroscopy (GC-HRMS) and FTIR analysis. The researchers focused on the extracts' anti-cancer potential. In order to find possible bioactive compounds with anticancer properties, the next step was to conduct an *in silico* molecular docking.

## MATERIALS AND METHODS

### Collection and authentication of Seaweeds

*Sargassum cinctum*, a brown marine seaweed that is a member of the Phaeophyceae family, was manually picked in October 2018 near Rameswaram in the Gulf of Mannar, Tamil Nadu, India. Dr. B.B. Chaugule, a former head of Savitribai Phule University in Pune, recognized and verified the collected samples.

The samples were brought to the laboratory in sterile bags after being thoroughly cleansed with seawater to get rid

of any unwanted material such as stones, epiphytes, shells, and sand particles. Following tap water and distilled water wash, the samples were spread out in a dark area to dry. The dried samples were then pulverized [23].

**Preparation of ethanolic extract**

In a mechanical grinder, a dried *S. cinctum* sample was ground into powder. The dried seaweed powder was macerated with 70% ethanol for 7 days, till thoroughly submerged, incubated, and filtered using Whatman filter paper. The supernatant was subsequently concentrated with a rotating vacuum evaporator while being maintained at 4°C [23–25].

**GC-HRMS analysis of *S. cinctum***

GC-HRMS has solidified its position as a major technology platform for secondary metabolite profiling [26]. Until yet, no research has been published on the potential chemical components of "*Sargassum cinctum*," according to a thorough examination of the literature on the seaweeds under consideration.

To analyze potential chemical components, the current study prepared an ethanolic extract and then separated and identified the chemicals by exposing them to GC-MS analysis.

*Sargassum cinctum* was analyzed using a GC-HRMS system at the Indian Institute of Technology (IIT), Sophisticated Analytical Instrument Facility (SAIF), Bombay, Maharashtra, India, to detect any active bioactive substances that were present.

A combined analysis that is better able to analyze bioactive compounds qualitatively and quantitatively was utilized, and it is a high-resolution mass spectrometer and gas chromatograph (GC-HRMS Agilent 7899 Jeol, Accu-TOF GCV of source EI/CI with Time-of-Flight Analyzer operated at Mass range 10–2,000 amu at mass resolution–6,000). A carrier gas with a purity of 99.999% was utilized, flowing at a constant rate of 1.0 ml/minute. A standardized non-polar class capillary column with an active phase (DB-1) measuring 30 m × 0.20 mm × 0.25 µm in length, diameter, and film thickness, respectively, was employed. In the split mode, 1 ml of the sample was injected at 1:10 ratios. A split ratio of 10 and a temperature of 260°C was employed in the split injection mode. With a mass (*M*/*z*) range of 40–650, a solvent cut-off time of 4.50 minutes, and ion source and interface temperatures of 230°C and 270°C, respectively, experiments were carried out in relative detection mode.

With a column flow of 1.21 ml/minute, a linear velocity of 39.7 cm/second, and a purge flow of 3 ml/minute, a linear flow control mode was employed. The run lasts for an hour in total. With a heating rate of 5°C/minute, the oven temperature was set at 40°C for the first 20 minutes, 220°C for the middle 20 minutes, and 260°C for the last 20 minutes. The relative peak area of each component in the chromatogram was used to compute the retention time for that component. The fragmentation patterns of mass spectra were compared with those found in the spectrometer database using the National Institute of Standards and Technology (NIST) mass spectral database [27].

**FT-IR analysis of *S. cinctum***

The 400–4,000 $cm^{-1}$ wavelength region was used for the transmittance FTIR study using a Perkin Elmer Spectrophotometer instrument, it was employed to find the distinctive peaks and their functional groups. The FTIR's peak values were noted. All results findings were confirmed twice [14,28]

***In vitro* cell viability test of *S. cinctum***

The National Centre for Cell Sciences in Pune, India provided the BC cell line (MCF-7) and lung cell line (A549). The cytotoxicity of extracts was evaluated by the yellow tetrazolium (3-(4, 5-dimethyl thiazolyl-2)-2, 5-diphenyltetrazolium bromide) (MTT) MTT analysis. This method is based on the reduction of MTT by the action of mitochondrial reductase enzyme present in live cells. The quantity of MTT to formazan decreased in extract-treated and untreated cells was inversely correlated with the number of viable cells, by dissolving the formazan in dimethyl sulfoxide (DMSO) and measuring absorbance readings, it was evaluated. In short, cells (1 × 105) were plated and cultured for 24 hours at 37°C in a humid environment using 96 well plates. The old media was emptied without disturbing the cells when the cells had finished incubating. After that, the cells were examined using different extract dosages (0, 100, 250, 500, and 1,000 microgram per ml) while keeping the plate in the same incubation condition. Following incubation, 100 µl of 5 mg/ml MTT reagent in phosphate-buffered saline was added to everyone well, and the plates were then left to sit at 37°C for another 24 hours. To dissolve the resultant formazan, 100 µl of DMSO was added. A multiwell plate reader was then used to measure the reactant solution's absorbance at a wavelength of 595 nm (Tecan Multimode Reader, Austria). The concentrations of the test sample were then measured, showing 50% cell death [1,20]

**Molecular docking**

Finding novel ligands for proteins with known structures is a critical stage in the development of structure-based medicines, and *in silico* molecular docking is one of the best tools for this process. To examine the binding characteristics of *S. cinctum*, *in silico* molecular docking was performed in the current investigation. The validity and reliability of biological testing are increased by studies utilizing molecular docking and modelling, which also show how drugs may interact with their receptor targets. It is a method for fitting two molecules into a 3D workspace that may also be used in computer-aided drug design and structural biology [29].

***Ligand preparation***

In the current investigation, the compounds identified in the ethanolic extract of *S. cinctum* GC-HRMS examination were utilized. Chemdraw was used to produce the two-dimensional structures, and the Frog 2 server was utilised to produce the compounds' 3D conformers in sdf format [18,30].

### *Protein preparation*

The target proteins were acquired from the Protein Data Bank (www.rcsb.org), including VEGFR (PDB id 4AG8) [31,32]and AXL kinase (PDB id 5U6B] [33]. and water molecules from the protein's crystal structure were eliminated. Axitinib and a macrocyclic inhibitor were used to co-crystallize the structural models of the VEGFR and AXL Kinase, respectively. For docking experiment verification, these inhibitors were removed from the complex and put in a separate file. Molecular docking and virtual screening were done using the apo-part of the PDB file without the inhibitor [18].

### *Molecular docking and virtual screening*

AutoDock 4.2 was used to accomplish virtual screening and molecular docking [34,35] which is utilized by PyRx [36]. Using PDBQT, all receptors and molecules were modified to conform to AutoDock's specifications. To guarantee that the whole active site was docked, the default size of the grid box was positioned around the co-crystallized inhibitor in the center. The Lamarkian genetic algorithm's default settings were utilized to build a pose prediction. As part of the validation process for the docking system, AutoDock's capacity to predict experimental binding mode was evaluated. Effective validation is considered to have an RMSD value of less than 2 Å between the predicted and crystallographic locations [37]. Crystallographic poses were very comparable to those anticipated by AutoDock, with RMSD values of 0.72 (for AXL Kinase) and 0.96 (for VEGFR).

### *Post virtual screening analysis*

During the simulated screening, the receptor protein's ideal binding poses were determined. Lower binding energies were used to determine the ideal binding pose. The interactions of the complexes in two dimensions were predicted using LigPlot+ [18,38]. PyMol was used to see the complexes in 3D.

## RESULT AND DISCUSSION

### GC-HRMS analysis of *S. cinctum*

The identification of the various bioactive compounds of *S. cinctum* was assisted using GC-HRMS.

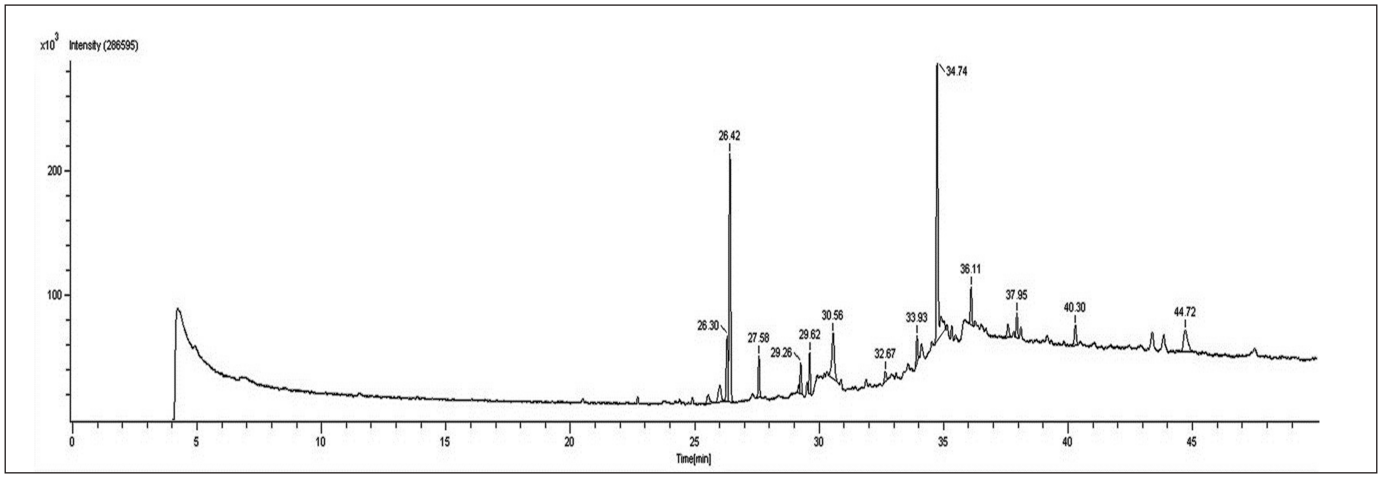


**Figure 1.** GC-HRMS spectrum of *S. cinctum*.

**Table 1.** A list of the bioactive substances discovered in *S. cinctum* using GC-HRMS analysis.

| Sr No | Name of the compound | Molecular Formula | MW | RT |
|---|---|---|---|---|
| 1. | 2-(16-Acetoxy-11-hydroxy-4,8,10,14-tetramethyl-3-oxohexadecahydrocyclopenta[a) phenanthren-17-ylidene)-6-methyl-hept-5-enoic acid, methylester | $C_{32}H_{48}O_6$ | 528 | 25.54 |
| 2. | 3-Pyridinecarboxylic acid, 2, 7, 10– tris (acetyloxy) 1,1a,2,3,4,6,7,10,11,11a-decahydro-1,1,3,6,9 pentamethyl-4-oxo-4a,7a-epoxy-5H-cyclopenta(a]cyclopropa | $C_{32}H_{39}NO_{10}$ | 597 | 26.02 |
| 3. | 2-(2-Diethylamino-ethoxy)- fluoren- 9-one | $C_{19}H_{21}NO_2$ | 295 | 26.30 |
| 4. | Hexadecanoic acid, ethyl ester | $C_{18}H_{36}O_2$ | 284 | 27.58 |
| 5. | 11-octadecenoic acid, methyl ester | $C_{19}H_{36}O_2$ | 296 | 29.26 |
| 6. | 7,8-Epoxylanostan-11-oL 3-acetoxy- | $C_{32}H_{54}O_4$ | 502 | 26.62 |
| 7. | 1b,4A Epoxy-2H-cyclopenta (3,4) cyclopropa (8,9) cycloundec (1,2-b) oxiren-5 (1 aH)- 1,2,7,9,10 telrakis (acetyloxy) decahydro-3,6,8,8,10a- pentamethyl | $C_{28}H_{38}O_{11}$ | 550 | 30.56 |
| 8. | Ethyl iso-allocholate | $C_{26}H_{44}O_5$ | 436 | 32.67 |
| 9. | 1,1′-Bicyclopropyl]-2-octanoic acid, 2′-hexyl-, methyl ester | $C_{21}H_{38}O_2$ | 322 | 37.95 |
| 10. | 9-0ctadecenoic acid, (2-phenyl-1,3-dioxolan 4-yl) methyl ester1,cis | $C_{28}H_{44}O_4$ | 444 | 40.29 |

Figure 1 illustrates the chromatograms for *S. cinctum*, and Table 1 lists the identified compounds from the GC-HRMS investigation. There were 10 peaks in total, and each peak indicated the bioactive chemicals that were seen by comparing its molecular formula, peak retention period, and molecular weight to those of the recognized compounds recommended by the NIST library. Mass spectrum of each compound isolated by GC-HRMS are depicted in Figures 2–8.

**FT-IR analysis of *S. cinctum***

After GC-HRMS analyses, the extract was processed for FT-IR analysis to identify the functional groups. Bioactives were found, according to FT-IR investigations. The FTIR analysis revealed several peaks that correspond to the functional groups found in the ethanol extract of *S. cinctum* as described in Figure 9.

The presence of free OH groups in phenolic compounds is indicated by a strong peak at 3,398.15. The presence of alkanes (-CH stretch) is indicated by the peak at 2,916.28. Ketone, aldehydes, and ester (C=O stretch) create the peak at 1,710.99 cm1. Alkenes (C=C-C stretch) are shown by the peak at 1,622.89, and the peak at 1,576.10 indicates the N-H primary amines. The alkene methylene group (C-H bending) is shown by the peak at 1,466.50, the peak at 1,377.20 (O-H) confirms the presence of phenol, the Peak due to ester at 1,157.30 (C-O-C), The peak at is caused by aliphatic amines (C-N stretch) at 1,037.27. The (N-H stretch) of amines created the peak at 932.15, and the peak at 721.23 (C-H Stretch) indicates alkanes.

***In vitro* cell viability test of *S. cinctum***

MCF7 and A549 cells were used to determine the extracts' cytotoxic potential. To assess their cytotoxic potential, *S. cinctum* extract was used at various concentrations (50, 100, 200, 500, and 750 µg/ml). Furthermore, the IC50 values for each extract were determined for the MCF-7 and A549 cell lines. As a control, cisplatin was utilised to test the effectiveness of these extracts.

*Sargassum cinctum* extracts inhibited MCF-7 and A549 cells significantly with IC50 134.50 and 161.02 µg/ml, respectively. The % cell inhibition in MCF 7 ranges from 42.91 to 89.07 while that of A549 is 38.11 to 89.5. Both the cell lines show % cell inhibition in a dose-dependent manner. *Sargassum cinctum* extracts show potent anticancer activity in MCF-7 and A549 cell lines when compared to standard cisplatin (Table 2 and Fig. 10).

**Statistical analyses**

The findings of all experiments were presented as the Mean ± Standard Deviation, with three independent replicates (Mean ± SD).

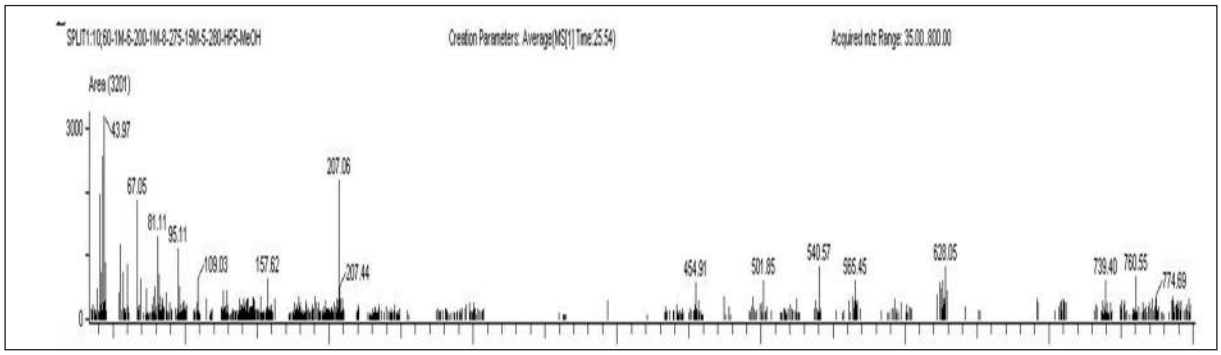


**Figure 2.** Mass spectrum of 2-(16-Acetoxy-11-hydroxy-4,8,10,14-tetramethyl-3 oxohexadecahydrocyclopenta [a) phenanthren-17-ylidene)-6-methyl-hept-5-enoic acid, methylester.

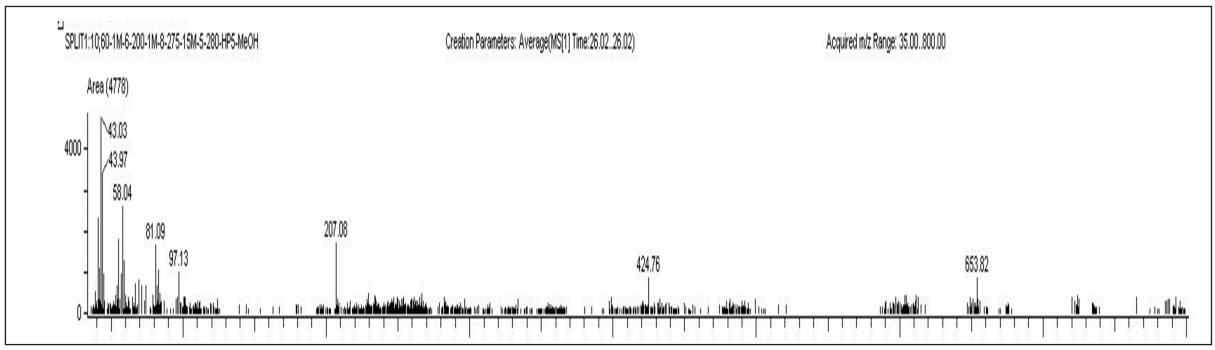


**Figure 3.** Mass spectrum of 3-Pyridinecarboxylic acid, 2, 7, 10 – tris (acetyloxy) 1,1a,2,3,4,6,7,10,11,11a-decahydro-1,1,3,6,9pentamethyl-4-oxo-4a,7a-epoxy-5H cyclopenta [a] cyclopropa.

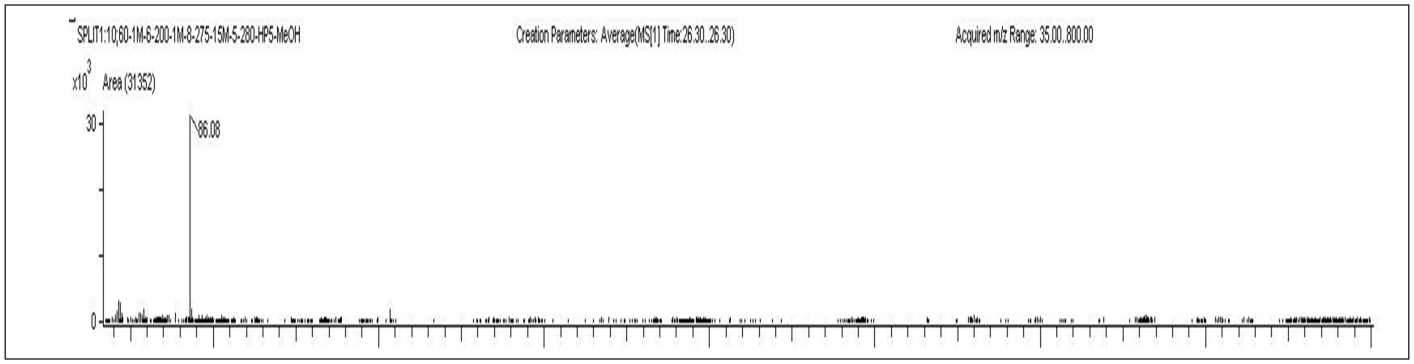


**Figure 4.** Mass spectrum of 2-(2-Diethylamino-ethoxy)- fluoren- 9-one.

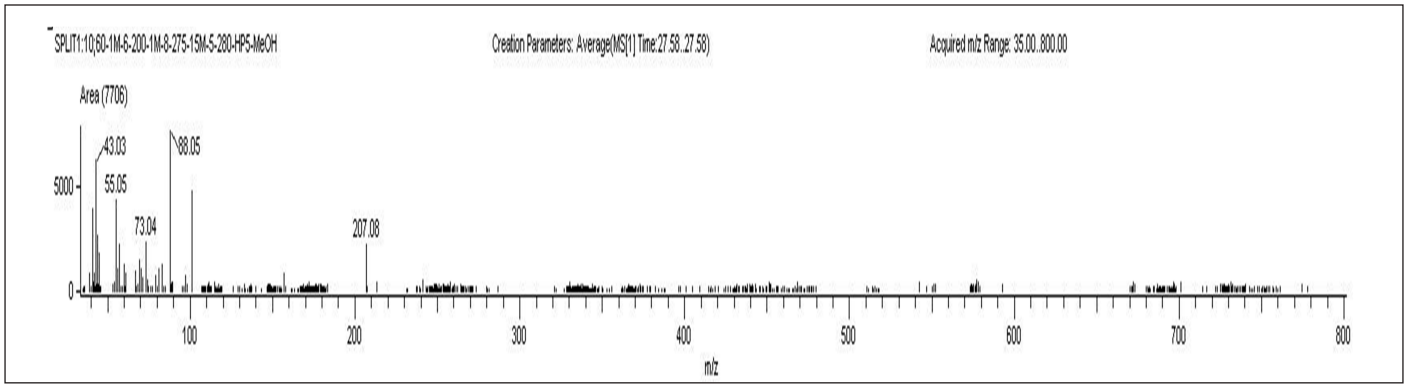


**Figure 5.** Mass spectrum of hexadecanoic acid, ethyl ester.

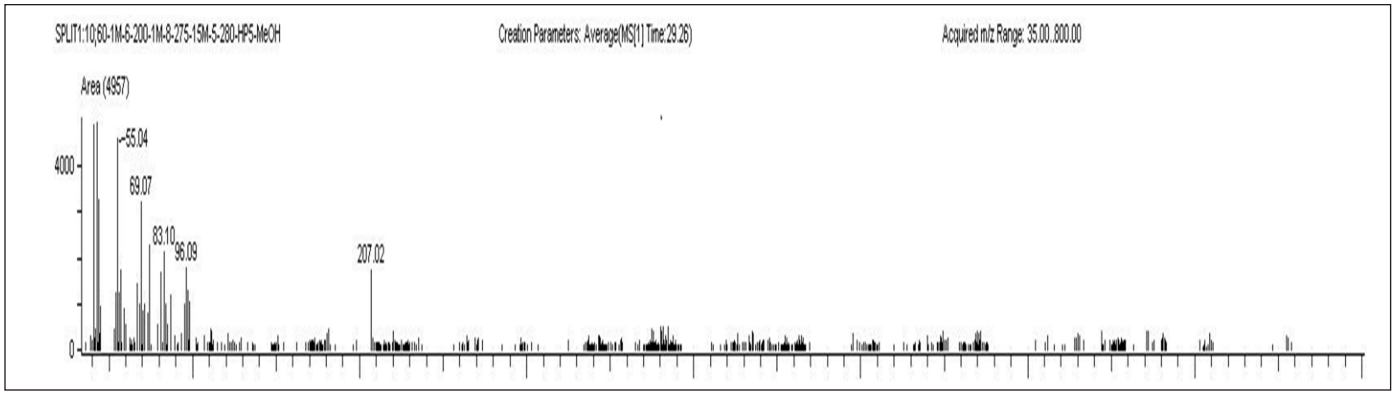


**Figure 6.** Mass spectrum of 11-octadecenoic acid, methyl ester.

**Molecular docking**

In comparison to the corresponding pharmacological inhibitors, molecular docking analysis revealed, there were significant interactions between the proteins and the phytochemicals. Tables 3 and 4 show the results of structural analysis and molecular docking of *S. cinctum* in the AXL kinase and VEGFR kinase domains, respectively.

***In-silico* study**

***Interactions of the metabolites from S. cinctum with AXL kinase***

The study findings regarding interactions with AXL kinase are shown in Table 3. Compounds 2-(16-Acetoxy-11-hydroxy-4,8,10,14-tetramethyl-3-oxohexadecahydrocyclopenta [a) phenanthren-17 ylidene) -6-methyl-hept-5-enoic acid, methyl ester from *S. cinctum*, is in polar interaction with Asp690's side chain. Asp690 is the first DFG loop residue in Axl Kinase Crystallographic studies [34] provided by suggested that this position plays a significant role in determining whether the enzyme is DFG-in or DFG-out, which affects whether the enzyme is catalytically active or inactive [18].

2-(2-Diethylamino-ethoxy)- fluoren- 9-one and 9-Octadecenoic acid, (2-phenyl-1,3- dioxolan 4-yl) methyl ester was shown to be involved in the polar contact with

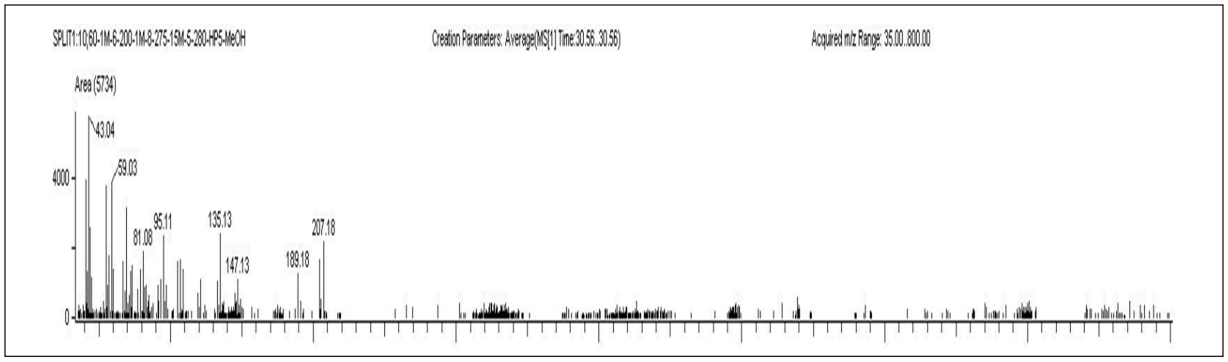


**Figure 7.** Mass spectrum of 1b,4A Epoxy-2H-cyclopenta (3,4) cyclopropa (8,9) cycloundec (1,2-b) oxiren-5 (1 aH)- 1,2,7,9,10 telrakis (acetyloxy) decahydro-3,6,8,8,10a- pentamethyl.

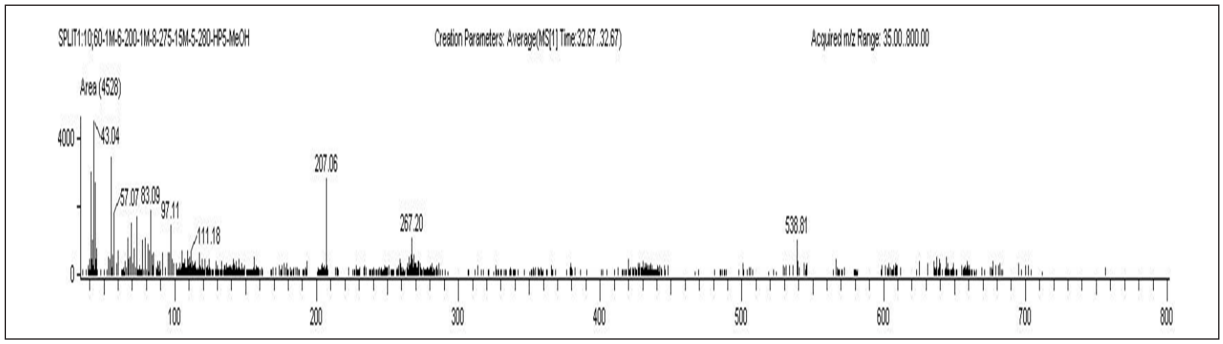


**Figure 8.** Mass spectrum of ethyl iso-allocholate.

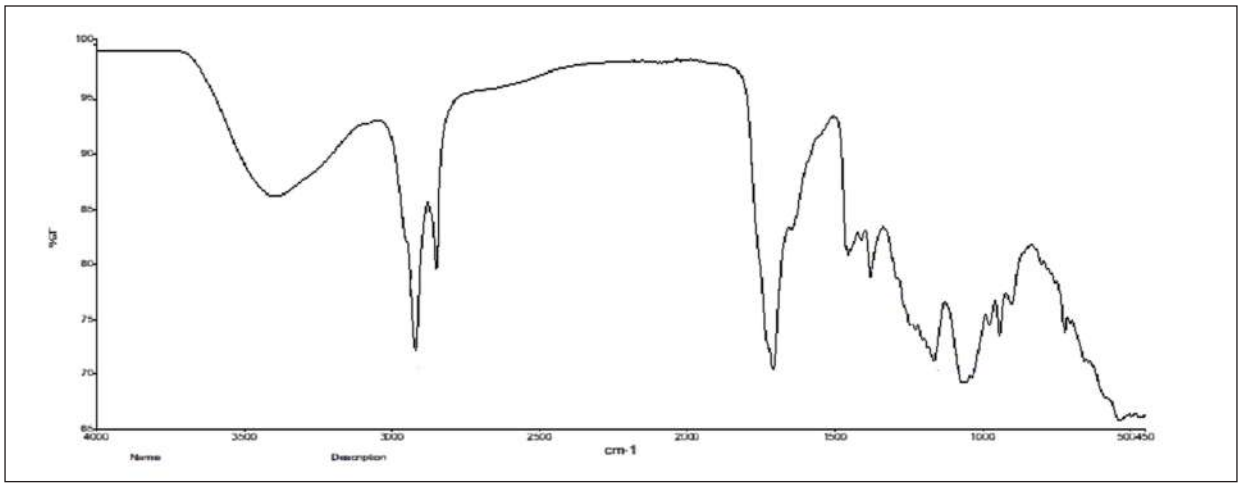


**Figure 9.** FT-IR spectrum of *S. cinctum*.

Met 623 of the hinge region [16]. Met623's side-chain and backbone atoms appear to be responsible for these interactions [18].

2-(16-Acetoxy-11-hydroxy-4,8,10,14-tetramethyl-3-oxohexadecahydrocyclopenta[a)phenanthren-17-ylidene)-6-methyl-hept-5-enoic acid, methylester, Hexadecanoic acid, ethylester, 11-octadecenoic acid, methyl ester, 7,8-Epoxylanostan-11-oL 3-acetoxy, Ethyl iso-allocholate, are found to create non-polar interaction with Met623.

2-(16-Acetoxy-11-hydroxy-4,8,10,14-tetramethyl-3-oxohexadecahydrocyclopenta[a)phenanthren-17-ylidene)-6-methyl-hept-5-enoic acid, methylester, 3-Pyridine carboxylic acid,2,7,10-tris (acetyloxy) -1, 1a, 2, 3, 4, 6, 7, 10, 11, 11a-decahydro-1,1,3,6,9 pentamethyl – 4 – oxo - 4a, 7a – epoxy - 5H-cyclopenta(a]cyclopropa, Hexadecanoic acid, ethylester, 11-octadecenoic acid, methyl ester, 1,1'-Bicyclopropyl]-2-octanoic acid, 2′-hexyl-, methyl ester were discovered to engaged in the polar interaction with Lys567 on an β-sheet of

N-lobe. Similarly, the compounds 2-(2-Diethylamino-ethoxy)-fluoren- 9-one, 7,8-Epoxylanostan-11-oL 3-acetoxy create a non-polar contact with Lys567 [18].

Therefore, such interaction of compounds 2-(16-Acetoxy-11-hydroxy-4,8,10,14-tetramethyl-3-oxohexadecahydrocyclopenta[a)phenanthren-17-ylidene)-6-methyl-hept-5-enoic acid, methylester, 3-Pyridine carboxylic acid,2,7,10-tris (acetyloxy) -1, 1a, 2, 3, 4, 6, 7, 10, 11, 11a-decahydro-1,1,3,6,9 pentamethyl – 4 – oxo - 4a, 7a – epoxy – 5H-cyclopenta(a]cyclopropa, Hexadecanoic acid, ethylester, 11-octadecenoic acid, methyl ester, 1,1'-Bicyclopropyl]-2-octanoic acid, 2'-hexyl-, methyl ester may have influenced the anti-cancer impact seen in the current study.

**Table 2.** Cell inhibition (%) and IC50 values for Sargassum cinctum extracts in comparison to MCF-7 and A549 cell lines.

| Conc µg/ml | MCF7 Cell-line | A 549 Cell-line | Cisplatin |
|---|---|---|---|
| 50 | 42.91 ± 0.89 | 38.11 ± 0.65 | 44.55 ± 1.1 |
| 100 | 48.31 ± 0.65 | 46.55 ± 0.85 | 49.94 ± 1.3 |
| 250 | 58.50 ± 1.2 | 59.79 ± 0.90 | 59.35 ± 0.65 |
| 500 | 74.79 ± 1.1 | 76.10 ± 1.1 | 75.35 ± 0.95 |
| 750 | 89.07 ± 0.98 | 89.5 ± 0.70 | 90.80 ± 1.2 |

All values are the mean of three replicates ± SD.

Figures 11 and 12 show the interactions between AXL Kinase and the metabolites from *S. cinctum*.

***Interactions of the metabolites from S. cinctum with VEGFR***

As shown in Table 4, the chemicals form active hydrogen bonds with Asn923, e.g., Asn923 forms hydrogen bonds with 7,8-Epoxylanostan-11-oL 3-acetoxy- from the *S. cinctum* sample, respectively. Similarly, the 2-(16-Acetoxy-11-hydroxy-4,8,10,14-tetramethyl-

**Table 3.** Findings acquired from docking and structural analysis of *S. cinctum* in the AXL kinase domain.

| Sr.no | Ligand (name) | Binding free energy (kcal/mol) | Hydrogen bonding pairs | Residues in hydrophobic interaction | Pi stacking interaction |
|---|---|---|---|---|---|
| 1 | 2-(16-Acetoxy-11-hydroxy-4,8,10,14-tetramethyl-3-oxohexadecahydrocyclopenta[a) phenanthren-17-ylidene)-6-methyl-hept-5-enoic acid, methylester | −4.15 | Lys567($NH^{SC}$): Lig (O), Asp690($OH^{SC}$): Lig (O), Asp627($O^{SC}$): Lig (OH) | Ala 689, Asp 690, Asp 627, Met 679, Asn 677, Arg 676, Gly 626, Val 550, Glu 544, Gly 545, Leu 620, Phe 622, Ala 565, Met 623, Leu 542 | |
| 2 | 3-Pyridinecarboxylic acid, 2, 7, 10 – tris (acetyloxy) 1,1a,2,3,4,6,7,10,11,11a-decahydro-1,1,3,6,9 pentamethyl-4-oxo-4a,7a-epoxy-5H-cyclopenta(a]cyclopropa | 1.78 | Asp627($NH^{BB}$): Lig (O), Lys567($NH^{SC}$): Lig (O) | Val 550, Leu 620, Phe 622, Met 679, Leu 542, Arg 676, Ala 565, Asp 690, Ala 689, Gly 626, Gly 543, Glu 544, Met 598 | |
| 3 | 2-(2-Diethylamino-ethoxy)- fluoren- 9-one | −8.4 | Met623($NH^{BB}$): Lig (O), | Val 550, Leu 542, Phe 622, Lys 567, Met 679, Arg 676, Ala 565, Leu 620, Asn 677, Asp 690, Ala 689 | Phe622: |
| 4 | Hexadecanoic acid, ethyl ester | −5.95 | Lys567($NH^{SC}$): Lig (O) | Met 598, Phe 622, Ala 689, Met 623, Met 679, Ala 565, Asp 627, Gly 626, Leu 620, Asp 690, Glu 585, Val 550, | |
| 5 | 11-octadecenoic acid, methyl ester | −5.82 | Lys567($NH^{SC}$): Lig (O) | Ala 565, Asp 690, Met 679, Leu 620, Val 550, Pro 621, Met 623, Met 598, Phe 622, Gly 626, Lys 624, Leu 542, | |
| 6 | 7,8-Epoxylanostan-11-oL 3-acetoxy- | −3.98 | Asn677($O^{SC}$): Lig (OH), Ser630($OH^{SC}$): Lig (O) | Ala 689, Asp 627, Ala 565, Asp 690, Asn 677, Phe 622, Gly 545, Glu 544, Arg 676, Lys 567, Met 623, Leu 542, Met 679, Met 598, Val 550 | |
| 7 | 1b,4A Epoxy-2H-cyclopenta (3,4) cyclopropa (8,9) cycloundec (1,2-b) oxiren-5 (1 aH)- 1,2,7,9,10 telrakis (acetyloxy) decahydro-3,6,8,8,10a-pentamethyl | 16.56 | No interaction | | |
| 8 | Ethyl iso-allocholate | −6.52 | Arg676($O^{SC}$): Lig (OH), Met679($S^{SC}$): Lig (OH) | Asp 690, Lys 624, His 625, Asn 677, Met 623, Gly 626, Met 598, Val 550, Met 679, Arg 676, Phe 622, Leu 542, Ala 565, Ala 689, Leu 620 | |
| 9 | 1,1'-Bicyclopropyl]-2-octanoic acid, 2'-hexyl-, methyl ester | −7.31 | Lys567($NH^{SC}$): Lig (O) | Met 679, Gly 543, Met 598, Ala 565, Leu 542 | |
| 10 | 9-0ctadecenoic acid, (2-phenyl-1,3-dioxolan 4-yl) methyl ester1,cis | −7.09 | Met623($NH^{BB}$): Lig (O) | Gly 626, Lys 624, Asp 627, Leu 620, His 625, Ala 565, Ser 630, Phe 622, Met 679, Val 550, Gly 543, Arg 676, Met 598, Leu 542, | |

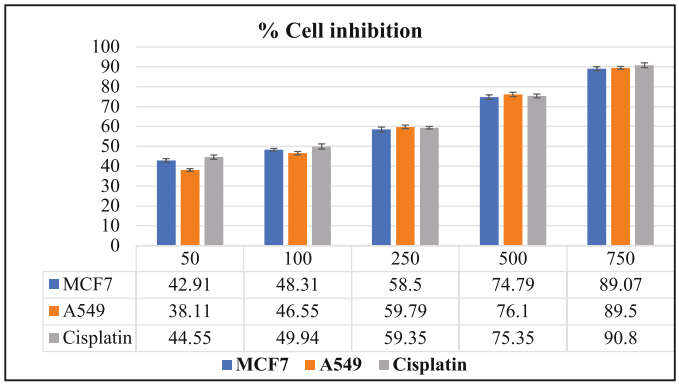


| | 50 | 100 | 250 | 500 | 750 |
|---|---|---|---|---|---|
| MCF7 | 42.91 | 48.31 | 58.5 | 74.79 | 89.07 |
| A549 | 38.11 | 46.55 | 59.79 | 76.1 | 89.5 |
| Cisplatin | 44.55 | 49.94 | 59.35 | 75.35 | 90.8 |

**Figure 10.** % Cell inhibition in MCF 7 and A549 cell-lines.

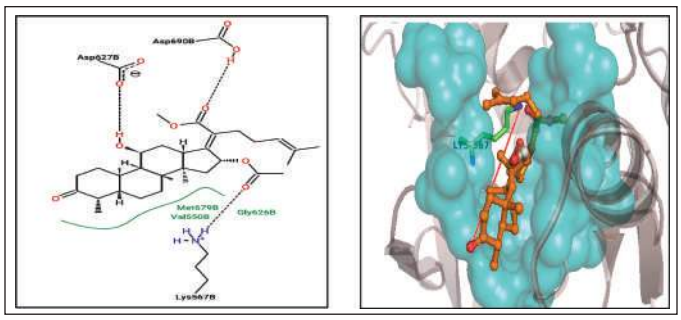

**Figure 11.** 2-(16-Acetoxy-11-hydroxy-4,8,10,14-tetramethyl-3-oxohexadecahydrocyclopenta [a)phenanthren-17-ylidene)-6-methyl-hept-5-enoic acid, methylester.

3-oxohexadecahydrocyclopenta[a) phenanthrene-17-ylidene)-6-methyl-hept-5-enoic acid, methyl ester. It has been reported that ethyl iso-allocholate and Asn923 create a non-polar contact. It is found that Asn923 side-chain and backbone atoms make up these interactions. It is interesting to note that Asn923 has been demonstrated to help suppress VEGFR in an experimental context. For instance, Harris *et al.* [39] studied a number of oxazole compounds for their ability to inhibit VEGFR and found that the compounds' sulfone functional group is oriented for effective inhibition by the polar and non-polar interactions from VEGFR . In most polar and non-polar interactions, Asn923 is involved. Considering that Asn923 plays a major role in VEGFR inhibitory function and that the current study found that a variety of phytochemicals interact with Asn923. Considering that Asn923 plays a major role in VEGFR inhibitory function and that the current study found that a variety of phytochemicals interact with Asn923. Therefore, it can be said that the phytochemicals that have been found may have contributed to the current anticancer effect by inhibiting VEGFR, which is mediated by contact with Asn923 [18].

It was discovered that bioactives and the VEGFR residue Asp1046 create polar interactions. The polar interaction between Asp1046 of VEGFR and 1,1′-Bicyclopropyl]-2-octanoic acid, 2′-hexyl-, methyl ester, 9-Octadecenoic acid, and (2-phenyl-1,3- dioxolan 4-yl)

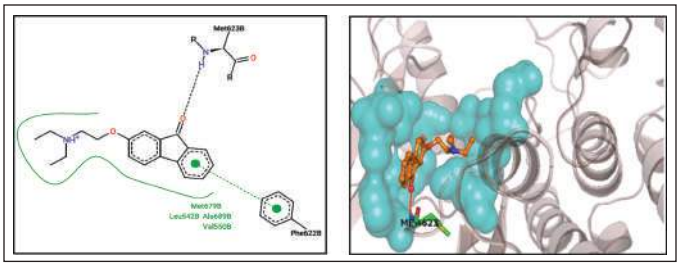

**Figure 12.** 2- (2-Diethylamino-ethoxy)-fluoren- 9-one.

methyl ester was discovered. These interactions involve both backbone atoms. Asp1046 of VEGFR forms a non-polar contact with hexadecanoic acid, ethyl ester, 11-octadecenoic acid, methyl ester, and ethyl iso-allocholate. The highly recognized DFG loop of VEGFR, which regulates the active and inactive states of the enzyme, starts with asp1046, the first residue [40,41]. Asp1046 interacts with the carbonyl group of known medications, such as benzimidazole, according to crystallographic descriptions [42]. A further analysis of amino-benzoxazole compounds revealed that the side chain of Asp1046 and the endocyclic nitrogen of the active functional group formed a robust hydrogen bond [43]. Based on the circumstantial literature and our study's results, we can confidently assume that the plant sample's exhibited anti-cancer action is mediated by phytochemicals interacting with VEGFR Asp1046 [18].

It is discovered that several active metabolites are present close to the Lys868 residue in both samples. For instance, Lys868 of VEGFR and 2-(2-Diethylamino-ethoxy)-fluoren-9-one, 11-octadecenoic acid, methyl ester, 1,1′-Bicyclopropyl]-2-octanoic acid, 2′-hexyl-, methyl ester, and 2-phenyl-1,3- dioxolan 4-yl) methyl ester have all been linked to non-polar interactions. It has been found that Lys868 plays a crucial part in how well anilino-aryloxazoles inhibit VEGFR [39]. This residue supervises the ribose sugar moiety of the nucleotide adenosine triphosphate being retained during catalysis. Mutants exhibiting complete loss of kinase activity were produced in artificial mutagenesis experiments when this lysine was replaced with methionine [44]. Lys868 is located in a crucial location where the nucleotide binds and influences ligand binding by supplying polar and non-polar interactions [39]. In the current docking data, we found that this residue contributes both polar and non-polarly to other phytoconstituents from both samples, which is consistent with the experimental results. As a result, from *S. cinctum* 2-(16-Acetoxy-11-hydroxy-4,8,10,14-tetramethyl-3-oxohexadecahydrocyclopenta[a)phenanthren-17-ylidene)-6-methyl-hept-5-enoic acid, methylester, 2-(2-Diethylamino-ethoxy)- fluoren- 9-one, 7,8-Epoxylanostan-11-oL 3-acetoxy, Ethyl iso-allocholate, 1,1′-Bicyclopropyl]-2-octanoic acid, 2′-hexyl-, methyl ester, 9-0ctadecenoic acid, (2-phenyl-1,3-dioxolan 4-yl) methyl ester may serve as strong inhibitors of VEGFR by interacting with residue Lys868 [18]. The interactions between VEGFR and the metabolites from *S. cinctum* were displayed in Figures 13 and 14.

**Table 4.** Information obtained from docking and structural analysis of *S. cinctum* in the VEGFR kinase domain.

| Sr.no | Ligand (name) | Binding free energy (kcal/mol) | Hydrogen bonding pairs | Residues in hydrophobic interaction |
|---|---|---|---|---|
| 1 | 2-(16-Acetoxy-11-hydroxy-4,8,10,14-tetramethyl-3-oxohexadecahydrocyclopenta[a]phenanthren-17-ylidene)-6-methyl-hept-5-enoic acid, methylester | −7.34 | Asn923($NH^{BB}$): Lig (OH) | Pro 839, Arg 842, Phe 918, Phe 1047, Lys 838, Gly 841, Leu 840, Glu 850, Lys 920, Asn 923 |
| 2 | 3-Pyridinecarboxylic acid, 2, 7, 10– tris (acetyloxy) 1,1a,2,3,4,6,7,10,11,11a-decahydro-1,1,3,6,9 pentamethyl-4-oxo-4a,7a-epoxy-5H-cyclopenta[a] cyclopropa | −6.81 | Asn923($NH^{BB}$): Lig (OH), Asn923($O^{SC}$): Lig (OH) | Phe 918, Leu 840, Gly 922, Phe 1047, Lys 920, Phe 921, Pro 839, Cys 919, Gly 841, Val 848, Leu 1035, |
| 3 | 2-(2-Diethylamino-ethoxy)- fluoren- 9-one | −6.2 | Cys919($NH^{BB}$): Lig (O) | Leu 840, Ala 866, Val 916, Leu 889, Phe 918, Glu 885, Lys 868, Val 914, Glu 917, Leu 840, Val 899, Cys 1045, Gly 922, Phe 1047, Leu 1035 |
| 4 | Hexadecanoic acid, ethyl ester | −3.12 | Cys919($NH^{BB}$): Lig (O) | Leu 889, Leu 1019, Ile 1044, Leu 840, Val 898, Glu 885, Phe 918, Asp1046, Cys 1045, Ala 866, Leu 1035, Val 848, Val 916, Gly 922, Val 899 |
| 5 | 11-octadecenoic acid, methyl ester | −2.98 | Cys919($NH^{BB}$): Lig (O) | Ala 866, Val 848, Glu 885, Val 914, Val 916, Leu 840, Lys 868, Cys 919, Leu 1035, Gly 922, Phe 1047, Asp 1046, Phe 918, Cys1045, Val 899 |
| 6 | 7,8-Epoxylanostan-11-oL 3-acetoxy- | −7.17 | Asn923($NH^{BB}$): Lig (OH), Asn923($O^{SC}$): Lig (OH) | Phe 1047, Gly 922, Gly 841, Leu 1035, Arg 842, Val 848, Leu 840, Ala 866 |
| 7 | 1b,4A Epoxy-2H-cyclopenta (3,4) cyclopropa (8,9) cycloundec (1,2-b) oxiren-5 (1 aH)- 1,2,7,9,10 telrakis (acetyloxy) decahydro-3,6,8,8,10a-pentamethyl | −5.93 | Cys919($NH^{BB}$): Lig (O) | Leu 1035, Ala 866, Phe 918, Arg 1032, Phe 1047, Lys 920, Phe 921, Gly 922, |
| 8 | Ethyl iso-allocholate | −6.82 | Leu840($O^{SC}$): Lig (OH) | Asp 1046, Phe 918, Val 848, Leu 840, Cys 919, Phe 1047, Gly 922, Val 899, Ala 866, Asn923, Cys1045, Glu 917, Leu 1035, Val 916, |
| 9 | 1,1′-Bicyclopropyl]-2-octanoic acid, 2′-hexyl-, methyl ester | −3.26 | Asp1046($NH^{BB}$): Lig (O) | Cys 1045, Lys 868, Ala 866, Val 848, Leu 840, Phe 1047, Leu 889, Leu 1035, Val 899, Val 914, Val 916, Gly 922, Cys 919, Glu 885, |
| 10 | 9-Octadecenoic acid, (2-phenyl-1,3- dioxolan 4-yl) methyl ester | −3.19 | Asp1046($NH^{BB}$): Lig (O) | Leu 889, Val 916, Lys 868, Ala 866, Cys 1045, Leu 840, Phe 918, Leu 1035, Gly 922, Val 848, Glu 885, Phe 1047 Val 899, Lys 920 |

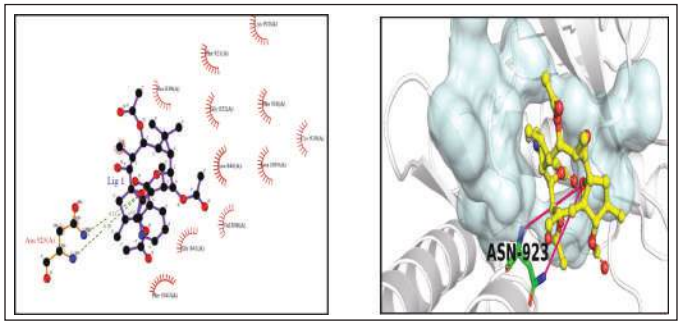


**Figure 13.** 3-Pyridinecarboxylic acid, 2, 7, 10 – tris (acetyloxy) 1,1a,2,3,4,6,7,10,11,11a-decahydro-1,1,3,6,9pentamethyl-4-oxo-4a,7a-epoxy-5H-cyclopenta[a]cyclopropa.

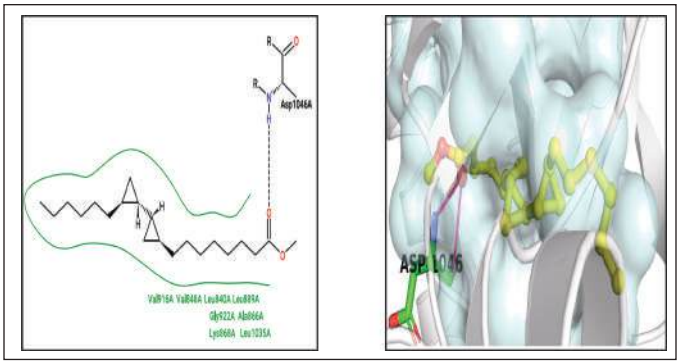


**Figure 14.** 1,1′-Bicyclopropyl]-2-octanoic acid, 2′-hexyl-, methyl ester.

## CONCLUSION

This study concluded that a variety of medicinal compounds may be found in seaweed that are both structurally and biologically active. The *Sargassum* species secondary metabolites may be the alleged potential biogenic metabolites for the manufacture of new medicines. According to this study, *Sargassum* extract contains a variety of bioactive substances

having a variety of biological properties, opening up new possibilities for future industrial applications.

To identify the bioactive substances in *S. cinctum*, a quick, easy, and effective technique based on molecular docking and GC-HRMS has been developed. The ethanol extract was analysed using GC-HRMS and FT-IR, which revealed the presence of several active compounds with potential medicinal uses. *In vitro* studies on the anticancer efficacy of the extract against breast and lung cancer cells revealed considerable dose-dependent cytotoxicity on tumour cell lines. In addition, the present work tries to shed light on the claimed mechanistic aspects of the anticancer activity of the provided seaweed samples using the structure interaction data gleaned from a molecular docking investigation. We speculate that the anti-cancer advantage shown in this study may have been influenced by residues such as Asn923, Phe1047, Lys868, and Asp1046 from VEGFR and Met623, Asp690, and Lys567 from AXL kinase. This is the first publication on the bioactive components of *S. cinctum* extracts that have anticancer potential, as far as we are aware.

## ACKNOWLEDGMENT

For the GC-HRMS experiments, the author wants to say thank you to the SAIF at IIT Bombay. The authors acknowledge the Biocyte Institute of Research and Development in Sangli, Maharashtra, for its *in vitro* anticancer activities. The authors thank the Savitribai Phule Pune University Bioinformatics Centre for their assistance with our molecular docking research.

## AUTHOR CONTRIBUTIONS

All authors made substantial contributions to conception and design, acquisition of data, or analysis and interpretation of data; took part in drafting the article or revising it critically for important intellectual content; agreed to submit to the current journal; gave final approval of the version to be published; and agree to be accountable for all aspects of the work. All the authors are eligible to be an author as per the International Committee of Medical Journal Editors (ICMJE) requirements/guidelines.

## FINANCIAL SUPPORT

The author(s) of this article claim that funding is not received for the study described in it.

## CONFLICTS OF INTEREST

The authors report no financial or any other conflicts of interest in this work

## ETHICAL APPROVALS

This study does not involve experiments on animals or human subjects.

## DATA AVAILABILITY

All data generated and analyzed are included in this research article.

## USE OF ARTIFICIAL INTELLIGENCE (AI)-ASSISTED TECHNOLOGY

The authors declares that they have not used artificial intelligence (AI)-tools for writing and editing of the manuscript, and no images were manipulated using AI.

## PUBLISHER'S NOTE

All claims expressed in this article are solely those of the authors and do not necessarily represent those of the publisher, the editors and the reviewers. This journal remains neutral with regard to jurisdictional claims in published institutional affiliation.

## REFERENCES

1. Ghate NB, Hazra B, Sarkar R, Mandal N. *In vitro* anticancer activity of *Spondias pinnata* bark on human lung and breast carcinoma. Cytotechnology. 2014;66:209–18. doi: https://doi.org/10.1007/s10616-013-9553-7
2. Salunke M, Wakure B, Wakte P. High-resolution liquid chromatography mass spectrometry (HR-LCMS) and 1H NMR analysis of methanol extracts from marine seaweed *Gracilaria edulis*. Nat Prod Res. 2024;38:1441–4. doi: https://doi.org/10.1080/14786419.2022.2146906
3. Hsu H, Hwang P. Clinical applications of fucoidan in translational medicine for adjuvant cancer therapy. Clin Transl Med. 2019;8:15. doi: https://doi.org/10.1186/s40169-019-0234-9
4. Falzone L, Salomone S, Libra M. Evolution of cancer pharmacological treatments at the turn of the third millennium. Front Pharmacol. 2018;9:1300. doi: https://doi.org/10.3389/fphar.2018.01300
5. Mofeed J, Deyab M, El A, Sabry N, Ward F. *In vitro* anticancer activity of five marine seaweeds extract from Egypt against human breast and colon cancer cell lines. Res Sq. 2021:1–15. doi: https://doi.org/10.21203/rs.3.rs-462221/v1
6. Liu G, Kuang S, Wu S, Jin W, Sun C. A novel polysaccharide from *Sargassum* integerrimum induces apoptosis in A549 cells and prevents angiogensis *in vitro* and *in vivo*. Sci Rep. 2016;6:26722. doi: https://doi.org/10.1038/srep26722
7. Van Weelden G, Bobi M, Okła K, van Weelden WJ, Romano A, Pijnenborg JMA. Fucoidan structure and activity in relation to anti-cancer mechanisms. Mar Drugs. 2019;17:32. doi: https://doi.org/10.3390/md17010032
8. Deepak P, Josebin MPD, Kasthuridevi R, Sowmiya R, Balasubramani G, Aiswarya D, *et al.* GC-MS metabolite profiling, antibacterial, antidiabetic and antioxidant activities of brown seawee activities of brown seaweeds, *Sargassum* wightii Greville Ex J. Agardh, 1848 and *Stoechospermum marginatum* (C. Agardh) Kützing 1843. Pharmacol Toxicol Biomed Rep. 2017;3:27–34. doi: https://doi.org/10.5530/ptb.2017.3.5
9. Balachandran P, Parthasarathy V, Ajay Kumar TV. Isolation of compounds from *Sargassum wightii* by GCMS and the molecular docking against anti-inflammatory marker COX2. Int Lett Chem Physics and Astronomy. 2016;63:1–12. doi: https://doi.org/10.18052/www.scipress.com/ilcpa.63.1
10. Ragunath C, Kumar YAS, Kanivalan I, Radhakrishnan S. Phytochemical screening and gc-ms analysis of bioactive constituents in the methanolic extract of *caulerpa* racemosa (Forssk.) j. agardh and padina boergesenii allender & kraft. Curr Appl Sci Technol. 2020;20:380–93. doi: https://doi.org/10.14456/cast.2020.24
11. Abdelrheem DA, Rahman AA, Elsayed KNM, Abd El-Mageed HR, Mohamed HS, Ahmed SA. Isolation, characterization, *in vitro* anticancer activity, dft calculations, molecular docking, bioactivity score, drug-likeness and admet studies of eight phytoconstituents from brown alga *sargassum platycarpum*. J Mol Struct. 2021;1225:129245. doi: https://doi.org/10.1016/j.molstruc.2020.129245

12. Karthick V, Akhila C, Ganesh Kumar V, Subashini D, Dhas TS, Govindaraju K, *et al. In vitro* anticancer activity of Sargassum sp. polysaccharides against MCF-7 cell lines. Indian J Geo Marine Sci. 2019;48:1267–73.
13. Fazeela Mahaboob Begum SPRSSH. Novel anticancerous compounds from *Sargassum* wightii: *in silico* and *in vitro* approaches to test the antiproliferative efficacy. J Adv Pharm Edu Res. 2017;7:272–7.
14. Salunke MA, Wakure BS, Wakte PS. High-resolution liquid chromatography and mass spectrometry (HR-LCMS) assisted phytochemical profiling and an assessment of anticancer activities of *Gracilaria foliifera* and *Turbinaria conoides* using *in vitro* and molecular docking analysis. J Biomol Struct Dyn. 2023;41(14):6476–91. doi: https://doi.org/10.1080/07391102.2022.2108495
15. Sarukhanyan E, Shityakov S, Dandekar T. Rational drug design of Axl tyrosine kinase type I inhibitors as promising candidates against cancer. Front Chem. 2020;7:920. doi: https://doi.org/10.3389/fchem.2019.00920
16. Fatima G, Loubna A, Wiame L, Azeddine I. *In silico* inhibition studies of AXL Kinase by Curcumin and its natural derivatives. J Appl Bioinforma Comput Biol. 2017;06:1–6.doi: https://doi.org/10.4172/2329-9533.1000142
17. Hartshorn MJ, Verdonk ML, Chessari G, Brewerton SC, Mooij WTM, Mortenson PN, *et al.* Diverse, high-quality test set for the validation of protein-ligand docking performance. J Med Chem. 2007;50:726–41. doi: https://doi.org/10.1021/jm061277y
18. Salunke M, Wakure B, Wakte P. HR-LCMS assisted phytochemical screening and an assessment of anticancer activity of *Sargassum Squarrossum* and *Dictyota dichotoma* using *in vitro* and molecular docking approaches. J Mol Struct. 2022;1270:133833. doi: https://doi.org/10.1016/j.molstruc.2022.133833
19. Nakhjavani M, Smith E, Yeo K, Palethorpe HM, Tomita Y, Price TJ, *et al.* Anti-angiogenic properties of ginsenoside rg3 epimers: *in vitro* assessment of single and combination treatments. Cancers. (Basel) 2021;13:2223. doi: https://doi.org/10.3390/cancers13092223
20. Shankar KG, Sebastian D, Fleming AT, Ignacimuthu S, Antony JP. *In vitro* and *in silico* anticancer effect of combined crude acetone extracts of *Plumbago zeylanica* L., *Limonia acidissima* L. and *Artocarpus* heterophyllus Lam. Synergy. 2017;5:15–23. doi: https://doi.org/10.1016/j.synres.2017.11.003
21. Ralte L, Khiangte L, Thangjam NM, Kumar A, Singh YT. GC–MS and molecular docking analyses of phytochemicals from the underutilized plant, *Parkia timoriana* revealed candidate anti-cancerous and anti-inflammatory agents. Sci Rep. 2022;12:3395. doi: https://doi.org/10.1038/s41598-022-07320-2
22. de Ruyck J, Brysbaert G, Blossey R, Lensink MF. Molecular docking as a popular tool in drug design, an *in-silico* travel. Adv Appl Bioinform Chem. 2016;9:1–11. doi: https://doi.org/10.2147/AABC.S105289
23. Salunke M, Wakure B, Wakte P. Phytochemical screening of marine brown algae *Sargassum squarrossum* Greville. Bull Env Pharmacol Life Sci. 2022;11:112–6.
24. Salunke M, Wakure B, Wakte P. Hyphenated techniques for the characterization of seaweed bioactive compounds. Res J Pharm Technol. 2023;16:4455–61. doi: https://doi.org/10.52711/0974-360X.2023.00727
25. Salunke MA, Wakure BS, Wakte PS. Phytochemical, UV-VIS, and FTIR analysis of *Gracilaria foliifera*. Res J Pharm Technol. 2023;16:1391–4. doi: https://doi.org/10.52711/0974-360X.2023.00229
26. Kanthal LK, Dey A, Satyavathi K, Bhojaraju P. GC-MS analysis of bio-active compounds in methanolic extract of *Lactuca runcinata* DC. Pharmacognosy Res. 2014;6:58–61. doi: https://doi.org/10.4103/0974-8490.122919
27. Sasikumar R, Das D, Saravanan C, Deka SC. GC-HRMS screening of bioactive compounds responsible for antimicrobial and antioxidant activities of blood fruit (*Haematocarpus* validus Bakh. F. Ex Forman) of North-East India. Arch Microbiol. 2020;202:2643–54. doi: https://doi.org/10.1007/s00203-020-01985-x
28. Marimuthu J, Essakimuthu P, Janakiraman N, Anantham B, Tharmaraj RJJM, Arumugam S. Phytochemical characterization of brown seaweed *Sargassum wightii*. Asian Pac J Trop Dis. 2012;2:S109–S113. doi: https://doi.org/10.1016/S2222-1808(12)60134-0
29. Patil KK, Meshram RJ, Barage SH, Gacche RN. Dietary flavonoids inhibit the glycation of lens proteins: implications in the management of diabetic cataract. 3 Biotech. 2019;9:47. doi: https://doi.org/10.1007/s13205-019-1581-3
30. Miteva MA, Guyon F, Tufféry P. Frog2: efficient 3D conformation ensemble generator for small compounds. Nucleic Acids Res. 2010;38:W622–7. doi: https://doi.org/10.1093/nar/gkq325
31. McTigue M, Murray BW, Chen JH, Deng YL, Solowiej J, Kania RS. Molecular conformations, interactions, and properties associated with drug efficiency and clinical performance among VEGFR TK inhibitors. Proc Natl Acad Sci U S A. 2012;109:18281–9. doi: https://doi.org/10.1073/pnas.1207759109
32. Kendre N, Salunke M, Wakure B, Wakte P. HR-LCMS based phytochemical analysis and anticancer activity of *Triumfetta rhomboidea* with molecular docking approach. J Appl Pharm Sci. 2024;14:209–19. doi: https://doi.org/10.7324/JAPS.2024.148412
33. Gajiwala KS, Grodsky N, Bolaños B, Feng J, Ferre RA, Timofeevski S, *et al.* The Axl kinase domain in complex with a macrocyclic inhibitor offers first structural insights into an active TAM receptor kinase. J Biol Chem. 2017;292:15705–16. doi: https://doi.org/10.1074/jbc.M116.771485
34. Huey R, Morris GM, Olson AJ, Goodsell DS. Software news and update a semiempirical free energy force field with charge-based desolvation. J Comput Chem. 2007;28:1145–52. doi: https://doi.org/10.1002/jcc.20634
35. Morris GM, Ruth H, Lindstrom W, Sanner MF, Belew RK, Goodsell DS, *et al.* Software news and updates AutoDock4 and AutoDockTools4: automated docking with selective receptor flexibility. J Comput Chem. 2009;30:2785–91. doi: https://doi.org/10.1002/jcc.21256
36. Dallakyan S, Olson AJ. Small-molecule library screening by docking with PyRx. Methods Mol Biol. 2015;1263:243–50. https://doi.org/10.1007/978-1-4939-2269-7_19
37. Ramírez D, Caballero J. Is it reliable to rake the molecular docking top scoring position as the best solution without considering available structural data? Molecules. 2018;23:1038. doi: https://doi.org/10.3390/molecules23051038
38. Laskowski RA, Swindells MB. LigPlot+: multiple ligand-protein interaction diagrams for drug discovery. J Chem Inf Model. 2011;51:2778–86. doi: https://doi.org/10.1021/ci200227u
39. Harris PA, Cheung M, Hunter RN, Brown ML, Veal JM, Nolte RT, *et al.* Discovery and evaluation of 2-anilino-5-aryloxazoles as a novel class of VEGFR2 kinase inhibitors. J Med Chem. 2005;48:1610–9. doi: https://doi.org/10.1021/jm049538w
40. Mctigue MA, Wickersham JA, Pinko C, Showalter RE, Parast CV, Tempczyk-Russell A, *et al.* Crystal structure of the kinase domain of human vascular endothelial growth factor receptor 2: a key enzyme in angiogenesis. Structure. 1999;7:319–30.
41. Regan J, Capolino A, Cirillo PF, Gilmore T, Graham AG, Hickey E, *et al.* Structure-activity relationships of the p38α MAP kinase Inhibitor 1-(5-tert-Butyl-2-p-tolyl-2H-pyrazol-3-yl)-3-[4-(2-morpholin-4-yl-ethoxy) naphthalen-1-yl] urea (BIRB 796). J Med Chem. 2003;46:4676–86. doi: https://doi.org/10.1021/jm030121k
42. Hasegawa M, Nishigaki N, Washio Y, Kano K, Harris PA, Sato H, *et al.* Discovery of novel benzimidazoles as potent inhibitors of TIE-2 and VEGFR-2 tyrosine kinase receptors. J Med Chem. 2007;50:4453–70. doi: https://doi.org/10.1021/jm0611051
43. Potashman MH, Bready J, Coxon A, Demelfi TM, DiPietro L, Doerr N, *et al.* Design, synthesis, and evaluation of orally active benzimidazoles and benzoxazoles as vascular endothelial

growth factor-2 receptor tyrosine kinase inhibitors. J Med Chem. 2007;50:4351–73. doi: https://doi.org/10.1021/jm070034i

44. Tomoko Takahashi SYCMS. A single autophosphorylation site on KDR/Flk-1 isessential for VEGF-A-dependent activation of PLC-gand DNA synthesis in vascular endothelial cells. Eur Mol Biol Organ. 2001;20:2768–78

**How to cite this article:**
Salunke M, Mane P, Kumbhar S, Balaji Wakure B. An evaluation of *Sargassum cinctum* anticancer properties utilizing *in vitro* testing and molecular docking, with assistance from GC-HRMS and FTIR. J Appl Pharm Sci. 2024;14(09):169-181.